Supplementary materials

Table S1. Zeta potential and conductivity of Y-CDs before and after the addition of AZM (mean±SD, n=3)

Sample	Zeta Potential (mV)	Conductivity (mS/cm)
Y-CDs	+8.96±0.26	0.365±0.003
Y-CDs–AZM complexes	-7.25±0.79	0.143±0.001

Table S2. Summary of FT-IR peak assignments and changes upon AZM addition.

Peak in Y-CDs (cm^{-1})	Peak in Y-CDs–AZM complexes (cm^{-1})	Change	Assignment	Mechanistic Implication
~3465 (broad)	~3450 (narrow)	Blue shift (~15 cm^{-1}), narrowing	O–H/N–H stretching	Reorganization of hydrogen bonding network; formation of directional hydrogen bonds between Y-CDs and AZM
—	~2925	New peak	C–H stretching (–CH_3, –CH_2–)	Characteristic peak of AZM alkyl chains; confirms successful binding of AZM onto Y-CD surface
~1666 (strong)	~1603 (weak)	Red shift (~63 cm^{-1}), intensity decrease	C=O/C=N stretching	Coordination or electrostatic interaction involving carbonyl groups; decreased electron cloud density
~1404 (weak)	~1385 (strong)	Red shift (~19 cm^{-1}), intensity increase	–COO^-/–SO_3^- symmetric stretching	Electrostatic attraction between negatively charged groups and protonated tertiary amine of AZM
~1243	—	Disappeared	C–O/C–N stretching	Functional groups involved in interaction; vibrational modes suppressed or coupled
—	~1112, ~1045 (doublet)	New peaks	C–O–C ether linkage/S=O stretching	Characteristic vibrations of AZM ether bonds and Y-CD sulfonic acid groups; interfacial binding
~850 (weak)	~680 (strong)	Red shift (~170 cm^{-1}), intensity increase	Aromatic C–H out-of-plane bending	π-π stacking between aromatic domains of Y-CDs and conjugated lactone ring of AZM

Table S3. Recovery experiments using paper-based smartphone platform in real samples.

Sample	Added (μmol/L)	Found (μmol/L)	RSD (%, n = 6)	Recovery (%)
Tap water	137.5	120.27	2.13	87.47
	162.5	138.95	3.21	85.51
	187.5	166.02	2.58	88.54
Pond water	137.5	119.10	2.15	86.61
	162.5	139.28	2.59	85.71
	187.5	157.81	3.04	84.17
Milk	137.5	100.35	4.17	72.98
	162.5	125.06	3.59	76.96
	187.5	127.66	4.03	68.08

Table S4. Reproducibility across different smartphone devices

Sample	Test instrument	Added (μmol/L)	B/G ratio	Found (μmol/L)	RSD (%, n = 6)	Recovery (%)
Tap water	iPhone 16Pro	137.5	1.0179	120.27	2.13	87.47
		162.5	1.0461	138.95	3.21	85.51
		187.5	1.087	166.02	2.58	88.54
	Xiaomi 13	137.5	1.0159	118.95	1.98	86.51
		162.5	1.0427	136.70	3.36	84.12
		187.5	1.0729	156.66	2.57	83.55
Pond water	iPhone 16Pro	137.5	1.0162	119.10	2.15	86.61
		162.5	1.0466	139.28	2.59	85.71
		187.5	1.0746	157.81	3.04	84.17
	Xiaomi 13	137.5	1.0147	118.84	2.16	85.92
		162.5	1.0416	135.93	2.51	83.65
		187.5	1.0675	153.13	2.87	81.67
Milk	iPhone 16Pro	137.5	0.9878	100.35	4.17	72.98
		162.5	1.0252	125.06	3.59	76.96
		187.5	1.0292	127.66	4.03	68.08
	Xiaomi 13	137.5	0.9890	101.13	4.01	73.55
		162.5	1.0078	113.56	3.69	69.88
		187.5	1.0217	122.79	4.18	65.49

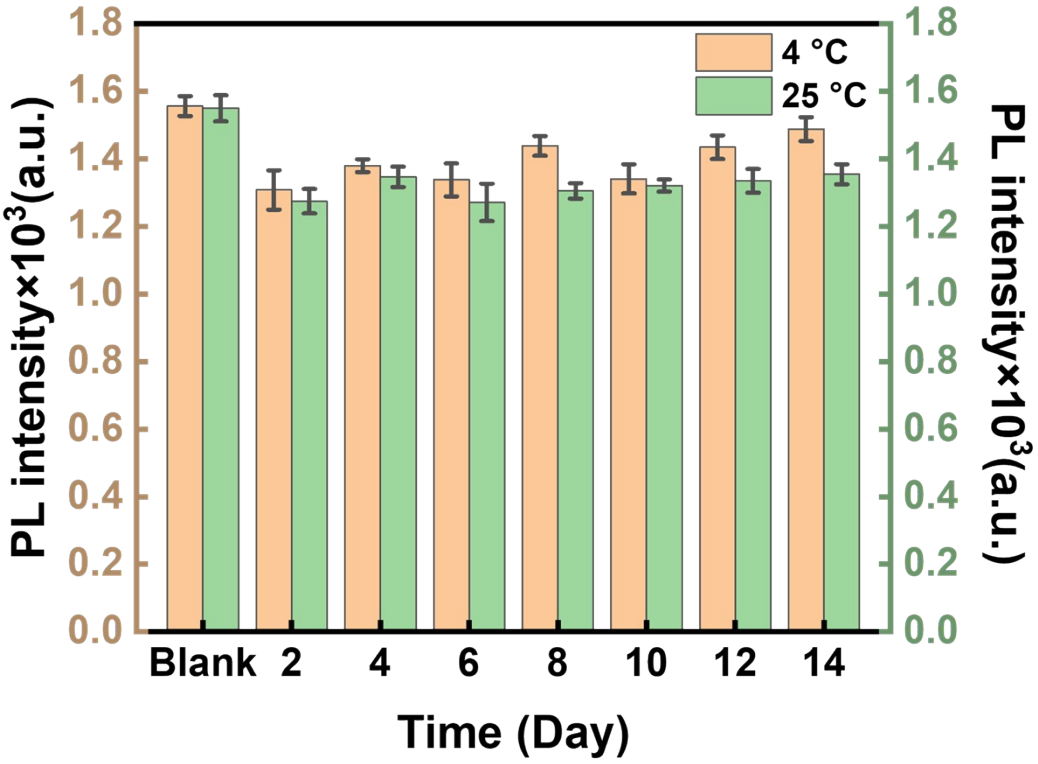

Figure S1. Stability of paper-based test strips stored under different conditions (4 °C and 25 °C) over 14 days.